

Topological phases protected by sublattice symmetry in dissipative quantum systems

Makio Kawasaki,¹ Ken Mochizuki,² and Hideaki Obuse^{1,3}

¹*Department of Applied Physics, Hokkaido University, Sapporo 060-8628, Japan*

²*Advanced Institute for Materials Research (WPI-AIMR), Tohoku University, Sendai 980-8577, Japan*

³*Institute of Industrial Science, The University of Tokyo,
5-1-5 Kashiwanoha, Kashiwa 277-8574, Japan*

Dissipative dynamics of quantum systems can be classified topologically based on the correspondence between the Lindbladian in the Gorini-Kossakowski-Sudarshan-Lindblad (GKSL) equation and the non-Hermitian Hamiltonian in the Schrödinger equation. While general non-Hermitian Hamiltonians are classified into 38 symmetry classes, the previous work shows that the Lindbladians are classified into 10 symmetry classes due to physical constraints. In this work, however, we unveil a topological classification of Lindbladians based on sublattice symmetry (SLS), which is not previously considered and can increase the number of symmetry classes for the Lindbladians. We introduce shifted SLS so that the Lindbladian can retain this symmetry and take on the same role of SLS for the topological classification. For verification, we construct a model of the dissipative quantum system retaining shifted SLS and confirm the presence of edge states protected by shifted SLS. Moreover, the relationship between the presence of shifted SLS protected edge states and dynamics of an observable quantity is also discussed.

I. INTRODUCTION

Recently, topological phases of non-Hermitian systems have attracted much attention [1–9]. The topological phases are classified by the presence or absence of symmetries, and non-Hermiticity of Hamiltonians enriches their symmetry class [10–12]. Moreover, non-Hermitian systems exhibit unique topological phenomena that have no counterpart in closed systems, non-Hermitian skin effects, and breakdown of the bulk-edge correspondence [13–17]. Non-Hermitian Hamiltonians describe certain types of open systems, for example, classical optical systems with gain and/or loss [18, 19], or postselected open quantum systems [20–22].

Whereas the Schrödinger equation with the non-Hermitian Hamiltonian describes short-time (*i.e.*, without quantum jumps) dynamics of a dissipative quantum system, it is necessary to consider the time-evolution of a density operator ρ for a long-time dynamics with quantum jumps. For a memoryless dissipative quantum system, the Gorini-Kossakowski-Sudarshan-Lindblad (GKSL) equation [23] $i\frac{d\rho}{dt} = \hat{\mathcal{L}}(\rho)$ describes the time-evolution of the density operator. The non-Hermitian superoperator called the Lindbladian $\hat{\mathcal{L}}$ completely characterizes the Markovian dynamics of the system. Accordingly, topological phases associated with the GKSL equation need to be considered in order to understand the topological phenomena of dissipative quantum systems. Nonequilibrium phenomena in dissipative many-body quantum systems have attracted attention recently [24–30]. In particular, the topological properties of steady states [31–36] and the spectra of Lindbladians [37–45] have been studied. Symmetry, which has a crucial role in topological classification, for Lindbladians is also investigated [46–51].

In particular, Ref. [41] studies the topological classification of the spectra of Lindbladians by using the

topological classification of non-Hermitian Hamiltonians. They suggest that the spectra of Lindbladians are classified into 10 symmetry classes, while non-Hermitian Hamiltonians are classified into 38 symmetry classes [12]. The absence of some symmetry classes originates from the fact that Lindbladians cannot possess certain types of symmetries which are used in the classification of non-Hermitian Hamiltonians due to physical constraints. We remark that although more than half of 38 symmetry classes for non-Hermitian Hamiltonians are classified by using sublattice symmetry (SLS), this symmetry is not considered in the previous work [41].

In this paper, we clarify the topological phases of Lindbladians originating from a modified version of SLS, which is not predicted in the previous tenfold classification [41]. To this end, we introduce shifted SLS which is defined by the combination of a constant shift of the spectrum of a Lindbladian and ordinary SLS. Whereas Lindbladians cannot retain ordinary SLS, Lindbladians can retain shifted SLS since the constant shift prevents violating the physical constraints. Thus, we reveal the topological classification of the Lindbladian which is previously unrecognized. To exemplify the topological phases originating from shifted SLS, we consider a Su-Schrieffer–Heeger (SSH) model with dissipation which retains shifted SLS and confirm the emergence of topological edge states protected by shifted SLS.

This paper is organized as follows. In Sec. II we review the spectrum of a Lindbladian and their topological classification. Then we define shifted SLS and explain that shifted SLS is a well-defined symmetry in dissipative quantum systems. We construct an SSH model with intra-sublattice dissipation which retains shifted SLS in Sec. III. We show that this model has edge states protected by shifted SLS, and they are robust against symmetry-preserving disorders. We also show that the emergence of the edge states affects the decay rate of the local occupation numbers. We summarize the results in

Sec. IV.

II. SYMMETRY CLASSES AND TOPOLOGICAL CLASSIFICATION OF LINDBLADIANS

A. GKSL equation and Lindbladians

We consider a quantum system coupled to environments. Assuming that the dynamics of the system is Markovian, the reduced density operator of the system ρ obeys the GKSL equation [23],

$$i\frac{d\rho}{dt} = \hat{\mathcal{L}}(\rho) = [\mathcal{H}, \rho] + i \sum_{\mu} (2L_{\mu}\rho L_{\mu}^{\dagger} - \{L_{\mu}^{\dagger}L_{\mu}, \rho\}). \quad (1)$$

The first term describes the unitary dynamics generated by a Hermitian Hamiltonian \mathcal{H} , and the second term describes the dissipative dynamics caused by non-Hermitian jump operators L_{μ} . The superoperator $\hat{\mathcal{L}}$ is called the Lindbladian. The solution of the GKSL equation (1) is formally described as

$$\rho(t) = \exp(-i\hat{\mathcal{L}}t)[\rho(0)], \quad (2)$$

in the similar manner as the Schrödinger equation.

Since Lindbladians are non-Hermitian linear superoperators, we can consider an eigenequation,

$$\hat{\mathcal{L}}[\rho_j] = \nu_j \rho_j, \quad \nu_j \in \mathbb{C}. \quad (3)$$

$-\text{Im} \nu_j$ corresponds to the decay rate of the eigenoperator ρ_j . To ensure that the solution of the GKSL equation given in Eq. (2) is a proper quantum state at any time t , the eigenvalues of general Lindbladians must satisfy the following two physical constraints. First, the imaginary part of eigenvalues is not positive because density operators are not amplified in time. Second, if there exists an eigenvalue ν , there also exists the eigenvalue $-\nu^*$ so that the solution of the GKSL equation be Hermitian.

B. Review of the tenfold classification of Lindbladians

We briefly review the topological classification of the spectra of Lindbladians studied in Ref. [41]. If the Hamiltonian describes non-interacting fermions and the jump operators are linear in fermionic operators, the corresponding Lindbladian also describes a non-interacting system. Then, we can classify the Lindbladian by using the classification of non-interacting non-Hermitian Hamiltonians [12].

First, we review the non-interacting Lindbladians and their description [52, 53]. For the dissipative non-interacting system of N fermions, the Hamiltonian and jump operators are expressed as

$$\mathcal{H} = \sum_{i,j}^{2N} w_i H_{i,j} w_j, \quad L_{\mu} = \sum_j l_{\mu,j} w_j, \quad (4)$$

where Hermitian operators w_j satisfy $\{w_i, w_j\} = 2\delta_{i,j}$ and are called Majorana operators. We note that the fermionic operators c and the Majorana operators are related as $c_j = (w_{2j-1} + iw_{2j})/2$. In such cases, the Lindbladian can be written as

$$\hat{\mathcal{L}} = 2(\hat{c}^{\dagger} \hat{c}) \begin{pmatrix} -Z^T & Y \\ 0 & Z \end{pmatrix} \begin{pmatrix} \hat{c} \\ \hat{c}^{\dagger} \end{pmatrix} - A_0 \hat{I}. \quad (5)$$

$\hat{c} = (\hat{c}_1 \hat{c}_2 \cdots \hat{c}_{2N})$ are fermionic superoperators satisfying $\{\hat{c}_i, \hat{c}_j^{\dagger}\} = \delta_{i,j}$, whose operation on ρ are defined by

$$\hat{c}_j[\rho] := \frac{1}{2}(w_j \rho + \hat{P}[\rho] w_j), \quad \hat{c}_j^{\dagger}[\rho] := \frac{1}{2}(w_j \rho - \hat{P}[\rho] w_j), \quad (6)$$

where $\hat{P} = e^{i\pi \sum \hat{c}_j^{\dagger} \hat{c}_j}$ is the parity superoperator, and \hat{I} denotes the identity superoperator. The matrices Z and Y are defined by

$$Z := H + i\text{Re}M, \quad Y := 2\text{Im}M, \quad (7)$$

where H and M are Hermitian $2N \times 2N$ matrices whose matrix elements are defined by $H_{i,j}$ in Eq. (4) and

$$M_{i,j} := \sum_{\mu} l_{\mu,i} l_{\mu,j}^*, \quad (8)$$

respectively. H has particle-hole symmetry $H = -H^*$ because of the anticommutation relation of the Majorana operators. The matrix M describes the effects of the dissipation and is called the bath matrix. The matrix Z becomes non-Hermitian when $\text{Re}M \neq 0$. A_0 is given as $A_0 = 2\text{tr}[M]$. If Z is diagonalizable, $\hat{\mathcal{L}}$ is also diagonalizable and the spectrum of the Lindbladian is completely determined by the spectrum of Z :

$$\hat{\mathcal{L}} = -4 \sum_j^{2N} \lambda_j \hat{b}'_j \hat{b}_j, \quad (9)$$

where λ_j are eigenvalues of Z . \hat{b}'_j and \hat{b}_j are generalized fermionic quasiparticles satisfying $\{\hat{b}_j, \hat{b}_k\} = \{\hat{b}'_j, \hat{b}'_k\} = 0$ and $\{\hat{b}_j, \hat{b}'_k\} = \delta_{j,k}$ [52].

Hence, we can focus on the topological classification of the non-Hermitian matrix Z instead of $\hat{\mathcal{L}}$ in order to classify the spectrum of the Lindbladian. We identify the symmetry classes of the Lindbladian through Z hereafter. Topological classification of Z is provided in Ref. [41], and the definition of symmetries in AZ and AZ^{\dagger} classes follows from Ref. [12]. Since the spectrum of the Lindbladian and Z are connected by Eq. (9), Z must have eigenvalues with positive imaginary parts. Due to this constraint, Z cannot have symmetries in AZ class and SLS. For example, if Z has time-reversal symmetry in AZ class, there exists a unitary operator \mathcal{T} such that $Z = \mathcal{T}^{-1}Z^*\mathcal{T}$. This equation ensures that Z has complex conjugate eigenvalue pairs. Then Z has eigenvalues with negative imaginary parts if Z has eigenvalues with finite

imaginary parts, which conflicts with the discussion in the previous subsection. Similarly, we can show that Z cannot retain SLS. If Z has SLS, there exists a unitary operator \mathcal{S} such that

$$Z = -\mathcal{S}^{-1}Z\mathcal{S}, \mathcal{S}^2 = 1. \quad (10)$$

This equation ensures that Z must have the eigenvalue $-\lambda$ if Z has an eigenvalue λ . This also conflicts with the physical constraints of the spectrum of the Lindbladian. We can show that other symmetries in the AZ class also generate the eigenvalues with negative imaginary parts, thus AZ symmetry is prohibited for Z . Consequently, Z can only have symmetries in AZ^\dagger class and Z is classified in tenfold symmetry classes which is the same number in the case of Hermitian Hamiltonians.

C. Shifted sublattice symmetry

While Lindbladians cannot retain ordinary SLS as explained below Eq. (10), we will show that a modified version of SLS, called shifted SLS, is permissible for the Lindbladians. We will also show that shifted SLS is topologically equivalent to the ordinary SLS.

Here, we introduce shifted SLS for a Lindbladian, which is the combination of a constant shift of the decay rate and ordinary SLS. Shifted SLS is defined by

$$Z' = -\mathcal{S}Z'\mathcal{S}^{-1}, \mathcal{S}^2 = I \quad (11)$$

$$Z' := Z - iaI, a := \frac{\text{tr}[Z]}{i\text{tr}[I]} \geq 0, \quad (12)$$

in real space and

$$Z'(\mathbf{k}) = -\mathcal{S}Z'(\mathbf{k})\mathcal{S}^{-1}, Z'(\mathbf{k}) := Z(\mathbf{k}) - iaI, \quad (13)$$

in momentum space, where I denotes the identity matrix whose dimension is same as Z . Shifted SLS ensures that Z has eigenvalue pairs $\pm\lambda + ia$. By definition of a in Eq. (12), the imaginary part of all eigenvalues of shifted SLS symmetric Z is positive, which satisfies the physical constraints for Lindbladians. Hence, shifted SLS can be retained for Lindbladians.

We remark that shifted SLS imposes the same topological constraints as ordinary SLS because the shifted SLS symmetric matrix can be continuously deformed into an SLS symmetric matrix without closing the gap and changing the symmetry class. Furthermore, Z' must inherit the same symmetries if Z retains some symmetries of AZ^\dagger class and vice versa. In other words, the topological phase of Z' corresponds to that of Z . Shifted SLS enables us to explore symmetry classes of Lindbladians which have not yet been studied in Ref. [41], that is, AZ^\dagger class with shifted SLS. Remarkably, among 38 fold classifications, 22 symmetry classes are related with SLS. This is the main result of the present work.

We also note that topological phases associated with pseudo-Hermiticity in Lindbladians can be realized in

a way similar to shifted SLS. While ordinary pseudo-Hermiticity $Z = \eta Z^\dagger \eta^{-1}$ conflicts the physical constraints for Lindbladians, shifted pseudo-Hermiticity

$$Z' = \eta Z'^\dagger \eta^{-1}, \eta^2 = I \quad (14)$$

is a valid symmetry for Lindbladians. We can investigate the topological phases protected by shifted pseudo-Hermiticity in dissipative quantum systems. Besides, PT symmetry, closely related to pseudo-Hermiticity, for Lindbladians is already defined in a shifted way in Ref. [46].

III. EXAMPLE : SSH MODEL WITH INTRA-SUBLATTICE DISSIPATION

In this section, we consider an SSH model with dissipation which retains shifted SLS and study its topological phase. In Sec. III A we explain the details of our model. We calculate topological invariants based on shifted SLS in Sec. III B. We numerically confirm the emergence of edge states and study their robustness against symmetry-preserving perturbation in Sec. III C. Finally, we investigate how edge states protected by shifted SLS affect the dynamics of the local occupation number in Sec. III D.

A. Model and symmetry

We consider the SSH model [54] with second nearest-neighbor coupling and dissipation, whose Lindbladian retains shifted SLS. The Hamiltonian is given by

$$\mathcal{H} = \sum_x \sum_{j=0}^2 (t_j c_{x,B}^\dagger c_{x+j,A} + \text{h.c.}), t_j \in \mathbb{R}, \quad (15)$$

where $c_{x,s}$ denotes the fermionic annihilation operator at position x with sublattice index $s \in \{A, B\}$. The jump operator is also given by

$$L_x = \gamma(c_{x,A} + c_{x,B}). \quad (16)$$

Non-negative number γ denotes the strength of the dissipation. The coupling strength between the system and environments does not depend on the position and the sublattice index. According to Sec. II B, we obtain the matrix Z by rewriting the fermionic annihilation operators at the site x on the sublattice s as the combination of Majorana operators $c_{x,s} = (w_{x,s,\alpha} + iw_{x,s,\beta})/2$,

$$Z = \begin{pmatrix} H^{\text{kit}} & 0 \\ 0 & -H^{\text{kit}} \end{pmatrix} + \frac{i\gamma^2}{4} \begin{pmatrix} I_2 & \sigma_x \\ \sigma_x & I_2 \end{pmatrix} \otimes \sum_x |x\rangle\langle x|, \quad (17)$$

where H^{kit} is the Majorana representation of the Kitaev chain Hamiltonian [55],

$$H_{xs,(x+j)\bar{s}}^{\text{kit}} = -H_{(x+j)\bar{s},xs}^{\text{kit}} = \frac{i}{4}t_j, \quad (18)$$

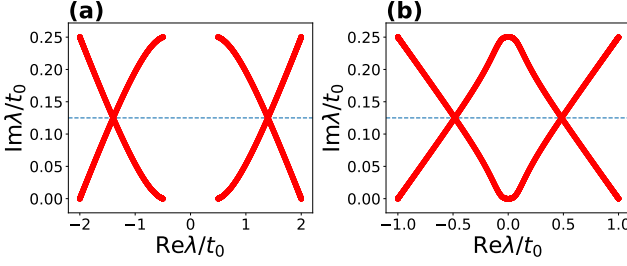


FIG. 1. Spectra of Z with periodic boundary condition with (a) $t_1 = 5t_0$, $t_2 = 2t_0$, and $\gamma^2 = 0.5t_0$, and (b) $t_1 = 2t_0$, $t_2 = t_0$, and $\gamma^2 = 0.5t_0$. The dashed lines in (a) and (b) indicate $\text{Im } \lambda = \frac{\gamma^2}{4}$.

and σ_x is one of the Pauli matrices. The second term in Eq. (17) describes the damping caused by the environments. Without dissipation ($\gamma = 0$), this term vanishes and the system is decomposed into the independent two Kitaev chains. On the other hand, dissipation realizes the dissipative coupling between two Kitaev chains, and the model can be interpreted as the ladder of the Kitaev chains with non-Hermitian couplings. Note that the order of the internal degree of freedom in Eq. (17) obeys $\{A\beta, B\alpha, A\alpha, B\beta\}$.

Under the periodic boundary conditions, the Fourier transform over the position space leads to the $Z(k)$ in the momentum space as

$$Z(k) = \frac{i}{4} \begin{pmatrix} \gamma^2 & -t_k^* & 0 & \gamma^2 \\ t_k & \gamma^2 & \gamma^2 & 0 \\ 0 & \gamma^2 & \gamma^2 & t_k^* \\ \gamma^2 & 0 & -t_k & \gamma^2 \end{pmatrix}, t_k = \sum_{j=0}^2 e^{ikj} t_j. \quad (19)$$

The eigenvalues of $Z(k)$ are calculated as

$$\lambda_{p,q}(k) = \frac{i\gamma^2}{4} + \frac{(-1)^q}{4} \sqrt{|t_k|^2 - \gamma^4 + (-1)^{p+1} 2i\gamma^2 \text{Ret}_k}, \quad (20)$$

where $p, q \in \{0, 1\}$. $Z(k)$ has a real line gap as shown in Fig. 1 (a), in a certain parameter region where topological phases are well defined. The gap closes for $\text{Ret}_k = 0$ and $|t_k|^2 \leq \gamma^4$. These conditions are satisfied in Fig. 1 (b), and the real line gap of Z closes.

According to Sec. II C, we focus on the traceless part of $Z(k)$,

$$Z'(k) := Z(k) - \frac{i\gamma^2}{4} I_4. \quad (21)$$

$Z'(k)$ has all symmetries of AZ † class, *i.e.*, time-reversal, particle-hole, and chiral symmetries,

$$Z'(k) = \mathcal{T} Z'^T(-k) \mathcal{T}^{-1}, \quad \mathcal{T} = \sigma_x \otimes I_2, \quad (22)$$

$$Z'(k) = -Z'^*(-k), \quad (23)$$

$$Z'(k) = -\Gamma Z'^\dagger(k) \Gamma^{-1}, \quad \Gamma = \mathcal{T}, \quad (24)$$

respectively. Moreover, $Z(k)$ has shifted SLS

$$Z'(k) = -\mathcal{S} Z'(k) \mathcal{S}^{-1}, \quad \mathcal{S} = I_2 \otimes \tau_z. \quad (25)$$

The Pauli matrices $\sigma_{x,y,z}$ and $\tau_{x,y,z}$ act on the sublattice and the block matrix spaces in Eq. (17), respectively. The symmetry operator of shifted SLS commutes with those of time-reversal symmetry in Eq. (22) and particle-hole symmetry in Eq. (23). According to the topological classification for non-Hermitian Hamiltonians [12], this model is belong to class $\text{BDI}^\dagger + \mathcal{S}_{++}$ (which is topologically equivalent to class $\text{BDI} + \mathcal{S}_{++}$), whose topological phase is classified in $\mathbb{Z} \oplus \mathbb{Z}$. This topological phase is not included in the prior classification of Lindbladians [41] because their classification misses the contribution of shifted SLS.

B. Topological invariant

$\mathbb{Z} \oplus \mathbb{Z}$ topological invariants can be calculated as follows [12]. $Z'(k)$ is pseudo-Hermitian by combining SLS and chiral symmetry,

$$Z'(k) = \eta Z'^\dagger(k) \eta^{-1}, \quad \eta = \Gamma \mathcal{S} = \sigma_x \otimes \tau_z. \quad (26)$$

Then $Z'(k)$ has block diagonal form $Z'(k) = \text{diag}\{Z'_+(k), Z'_-(k)\}$, and each subspaces are spanned by the biorthogonal vectors $|\phi_n^\pm\rangle$ and $|\phi_n^\pm\rangle$. These vectors are defined by

$$\eta |\phi_n^\pm\rangle = \pm |\phi_n^\pm\rangle. \quad (27)$$

Since $Z'_\pm(k)$ has SLS $Z'_\pm(k) = -\mathcal{S}_\pm Z'_\pm(k) \mathcal{S}_\pm^{-1}$, we can calculate the winding numbers

$$w_\pm := \frac{1}{4\pi i} \int_{\text{BZ}} dk \text{tr} \left[\mathcal{S}_\pm Z'^{-1}_\pm(k) \frac{dZ'_\pm(k)}{dk} \right] \quad (28)$$

for each subsector.

We find that two topological invariants coincide in our model, detailed discussion is provided in Appendix A. The topological invariant is given as

$$w = \frac{1}{2\pi i} \int_{\text{BZ}} dk \left[\frac{d}{dk} \log(t_k^* - i\gamma^2) + \frac{d}{dk} \log(t_k^* + i\gamma^2) \right]. \quad (29)$$

w corresponds to the sum of the winding number of two complex functons $t_k^* \pm i\gamma^2$. The parameters t_1 and t_2 dependence of the topological invariant w is shown in Fig. 2.

C. Bulk-edge correspondence

In this subsection, we numerically diagonalize Z and show the existence of the edge states [56]. We impose the open boundary conditions on the Hamiltonian in Eq. (15), and correspondingly there are two boundaries at each end in the system. Figure 3 shows spectra and edge states of Z with open boundary conditions. We observe four edge states in Fig. 3(a) whose parameters give $w = -2$ when periodic boundary conditions are imposed

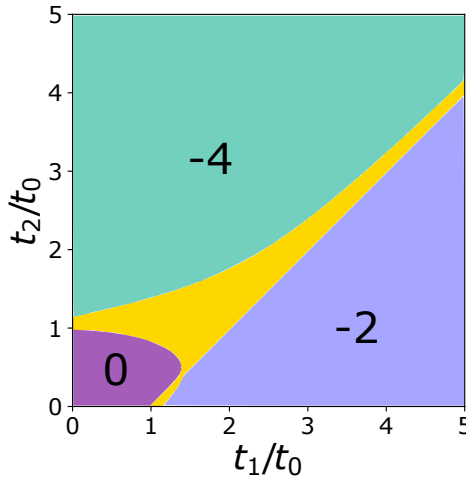


FIG. 2. Phase diagram of the topological invariant w for the dissipative SSH model with the second nearest neighbor coupling. We set the strength of dissipation $\gamma^2 = 0.5t_0$. In the yellow region, the real line gap closes and the winding number cannot be defined.

on the system. Because of the two boundaries of the system, this result verifies the bulk-edge correspondence. Since Z and Z' are related as Eq. (21) and the eigenvalue of the edge states of Z' is zero due to SLS, the edge states are the eigenstates of Z with eigenvalue $\frac{i\gamma^2}{4}$. In fact, the eigenvalues of edge states of non-interacting Lindbladians with shifted SLS are generally degenerated when the topological invariant is larger than one. The edge states are localized near boundaries as shown in Fig. 3 (b).

We also study the robustness of the edge states. We impose spatial disorder on hopping amplitudes. The hopping amplitude between (x, B) and $(x+j, A)$ are given as $t_{x,j} = \bar{t}_j + \delta t$, where \bar{t}_j is a mean value of $t_{x,j}$ and δt obeys the uniform distribution in the range $[-0.3t_0, 0.3t_0]$. The edge states will be robust against the disorder because the disorder does not break any symmetry on Z including shifted SLS. Figure 3(c) shows the spectrum of Z with the disorder. In this parameter $w = -4$ and eight edge states should appear. In Fig. 3(c) eight edge states appear, and the edge states are robust despite the bulk states being perturbed by the disorder. We note that the edge states may not be robust against the spatial disorder on γ . Although such disorder does not break any AZ^\dagger symmetry, the disorder breaks shifted SLS and changes the symmetry class of Z .

Finally, we numerically check the number of edge states in a wide range of t_1 and t_2 to confirm the bulk-edge correspondence and show the result in Fig. 4. The boundary of each color indicating the different number of edge states in Fig. 4 shows the almost same shape as Fig. 2. The number of edge states equals $2|w|$ in the whole region because of the two boundaries in the system. Hence, we verify that the winding number originated from shifted SLS corresponds with the number of edge states.

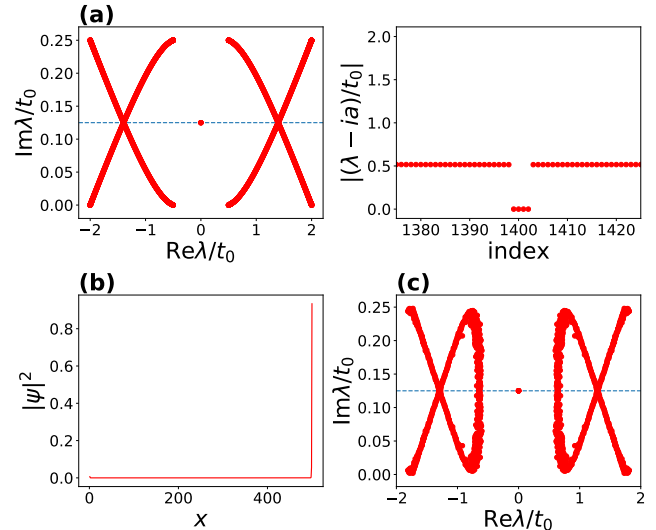


FIG. 3. (a) The spectrum of Z with open boundary conditions with $N = 500$, $t_1 = 5t_0$, $t_2 = 2t_0$, and $\gamma^2 = 0.5t_0$. Left: The spectrum on a complex plane. Right: The absolute value of the spectrum near $ia = i\gamma^2/4$. The horizontal axis represents the order of the eigenvalues. The four degenerated eigenstates appear at $\lambda = i\gamma^2/4$. (b) The spatial distribution of an edge state. We plot $|\psi|^2$ as $|\psi_x|^2 := \sum_{s=A,B} \sum_{\mu=\alpha,\beta} |\psi_{x,s,\mu}|^2$. (c) the spectrum of Z with random hopping with $t_1 = 2t_0$, $t_2 = 4t_0$, and $\gamma^2 = 0.5t_0$. The dashed lines in (a), and (c) indicate $\text{Im } \lambda = \frac{\gamma^2}{4}$.

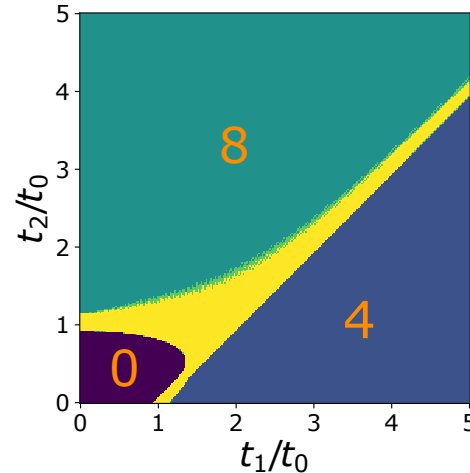


FIG. 4. Number of the edge states as a function of t_1 and t_2 . The band gap closes and the winding number cannot be defined in the yellow region.

D. Dynamics of local occupation number

Here, we clarify how the edge states in Z affect the time-evolution of the density operator. Since the physical meaning of fermionic superoperator \hat{c} defined in Eq. (6) is unclear, we focus on the dynamics of the local occupation

number [38] defined as

$$n_{x,s}(t) := \text{tr}[\rho(t)c_{x,s}^\dagger c_{x,s}], \quad (30)$$

where $c_{x,s}$ is the system's fermion appearing in Eq. (15).

First, we derive an analytical solution of the local occupation number $n_{x,s}(t)$. The local occupation number $n_{x,s}(t)$ can be rewritten as

$$n_{x,s}(t) = \frac{1}{2} - \frac{i}{2} \text{tr}[\rho(t)w_{x,s,\alpha}w_{x,s,\beta}]. \quad (31)$$

For non-interacting systems, the covariance matrix defined by $C_{j,k}(t) := \text{tr}[\rho(t)w_j w_k] - \delta_{j,k}$ obeys

$$\frac{dC}{dt} = 4i(Z^T C + CZ + Y). \quad (32)$$

If the system reaches a steady state ($\frac{d\rho}{dt} = 0$), the covariance matrix of the steady state C^{ss} satisfies [53]

$$Z^T C^{\text{ss}} + C^{\text{ss}} Z = -Y. \quad (33)$$

Focusing on the discrepancy with the steady state $\tilde{C}(t) = C(t) - C^{\text{ss}}$, $\tilde{C}(t)$ is explicitly expressed as

$$\tilde{C}(t) = e^{4iZ^T t} \tilde{C}(0) e^{4iZt}. \quad (34)$$

Inserting this solution to Eq. (31), we obtain the analytical solution of $n_{x,s}(t)$. In particular, we focus on the discrepancy with the steady state $n_{x,s}(t) - n_{x,s}^{\text{ss}}$, where $n_{x,s}^{\text{ss}} := \text{tr}[\rho^{\text{ss}} c_{x,s}^\dagger c_{x,s}]$ and $\mathcal{L}[\rho^{\text{ss}}] = 0$. This quantity is provided as

$$\begin{aligned} n_{x,s}(t) - n_{x,s}^{\text{ss}} &= -\frac{i}{2} \text{tr}[\rho(t)w_{x,s,\alpha}w_{x,s,\beta}] + \frac{i}{2} \text{tr}[\rho^{\text{ss}} w_{x,s,\alpha}w_{x,s,\beta}] \\ &= -\frac{i}{2} [\tilde{C}(t)]_{xs\alpha, xs\beta}. \end{aligned} \quad (35)$$

We plot $n_{x,s}(t) - n_{x,s}^{\text{ss}}$ in Fig. 5. From Eqs. (34) and (35), the local occupation number should decay as

$$n_{x,s}(t) - n_{x,s}^{\text{ss}} \propto e^{-8\text{Im}\tilde{\lambda}t}, \quad (36)$$

where $\tilde{\lambda}$ denotes an eigenvalue of Z whose eigenstate has largest overlap with $\rho(t)$. Since edge states, if exist, are localized near the boundary, the short-time dynamics of $n_{1,A}(t)$ and $n_{N,B}(t)$ clearly reflect the lifetime of the edge states. In those cases $\tilde{\lambda} = \frac{i\gamma^2}{4}$ and they decay as

$$n_{\text{edge}}(t) - n_{\text{edge}}^{\text{ss}} \propto e^{-2\gamma^2 t}. \quad (37)$$

This behavior depends only on the presence of edge states, but neither on the number of edge states nor detailed values of hopping amplitudes. As shown later, this behavior is derived from shifted SLS. In Fig. 5(a), the local occupation number near the boundaries have the same decay rate regardless of positions and the number

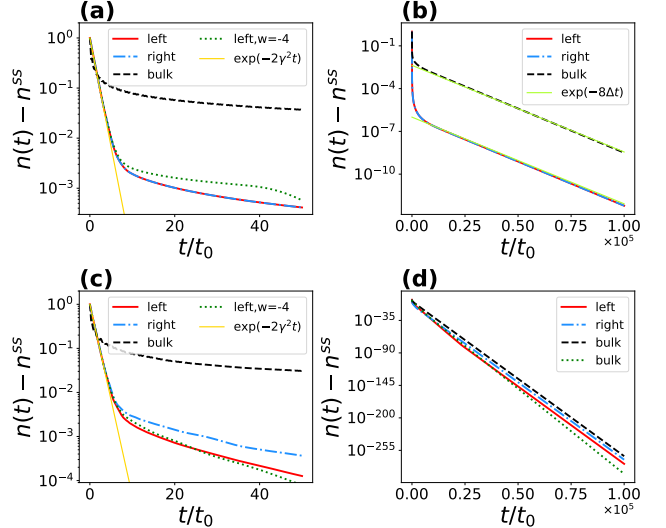


FIG. 5. Time evolution of the local occupation number $n_{x,s}(t)$. The labels (left, right, and bulk) in each figure denote the local occupation number at $(x, s) = (1, A)$, (N, B) and $(\frac{N}{2}, A)$, respectively. We set $N = 100$, $t_1 = 5t_0$, $t_2 = 2t_0$, and $\gamma^2 = 0.5t_0$ ($w = -2$) in this figure, except for "left, $w = -4$ " in (a) and (c). The initial states for each label are $\rho_{in} = |x, s\rangle \langle x, s|$, where $|x, s\rangle := c_{x,s} |\text{vac}\rangle$. (a) Short-time dynamics. We set $t_1 = 2t_0$, $t_2 = 4t_0$ ($w = -4$) in the green dotted line. (b) Long-time dynamics. $\Delta = 1.8 \times 10^{-5} t_0$ in this case. (c) Short-time dynamics with disorder. (d) Long-time dynamics with disorder. The green dotted line is calculated with different configuration of disorder. In (c) and (d), we induce the disorder in the same way as subsec. III C.

of edge states, which is consistent with Eq. (37). In contrast to short-time dynamics, the decay rate of long-time dynamics is determined from the spectral gap

$$\text{Im}\tilde{\lambda} = \Delta := \min_i \text{Im}\lambda_i. \quad (38)$$

As a consequence, $n_{x,s}(t)$ have same decay rate $8\Delta = 1.4 \times 10^{-4} t_0$ ($\Delta = 1.8 \times 10^{-5} t_0$) irrespective of their position or sublattice index, as shown in Fig. 5 (b).

Since the lifetime of the edge states is protected by shifted SLS, the decay rate of $n_{1,A}(t)$ and $n_{N,B}(t)$ are robust for symmetry-preserving disorders. This result is presented in Fig. 5(c). The decay rate of edge occupation numbers obeys Eq. (37) even in the presence of randomness. On the other hand, the spectral gap defined in Eq. (38) is not topologically protected. We plot the long-time dynamics of $n_{x,s}(t)$ with disorder in Fig. 5(d). The spectral gaps with different disorder configurations, plotted as black and green lines in Fig. 5(d), are $\Delta = 5.8 \times 10^{-4} t_0$ and $7.5 \times 10^{-4} t_0$, respectively. Correspondingly, bulk occupation numbers have different decay rates depending on the value of random hopping amplitudes, as shown in Fig. 5(d). Then we conclude that the decay rate for long-time dynamics depends on the configuration of hopping amplitudes.

We have seen that the lifetime of the edge occupation

number in short-time dynamics is given by the function of γ and does not depend on the realization of hopping amplitude $\{t_{x,j}\}$. In general, the lifetime of the edge occupation number in the presence of edge states only depends on the parameters of dissipation if the Lindbladian retains shifted SLS and particle-hole symmetry in AZ^\dagger class. The eigenvalues of edge states are given by $ia = \text{tr}[Z]/\text{tr}[I]$ from Eqs. (11) and (12). While Z contains the Hermitian Hamiltonian H and the bath matrix M , only the bath matrix M contributes to a since H has particle-hole symmetry $H^* = -H$ and then H is traceless. Therefore, we conclude that a , characterizing the lifetime of the edge occupation numbers, does not depend on the parameters of the Hamiltonian H in general. We also note that the decay rate of the edge occupation number n_{edge} for both ends coincides if the system has shifted SLS (*cf.* Ref. [38]), since shifted SLS guarantees the degeneracy of the eigenvalues of edge states and then $\tilde{\lambda}$ in Eq. (38) coincides for both ends.

IV. SUMMARY

In this work, we have introduced shifted SLS for Lindbladians and investigated the topological phase associated with shifted SLS. As a consequence, we have uncovered the new symmetry classes of Lindbladians, that is, AZ^\dagger with shifted SLS classes. Therefore, shifted SLS can increase the number of symmetry classes of Lindbladians. We have constructed the dissipative version of the SSH model retaining shifted SLS and confirmed the presence of edge states protected by shifted SLS. We have also studied the dynamics of the local occupation numbers and clarified that the edge occupation numbers have a universal decay rate which is also protected by shifted SLS for short-time dynamics. Our work open up an arena to the study of nonequilibrium topological phenomena in dissipative quantum systems.

ACKNOWLEDGEMENTS

We thank Yasuhiro Asano, Masatoshi Sato, and Kousuke Yakubo for helpful discussions. M. K. was supported by DX Doctoral Fellowship (Grant No. JP-MJSP2119) from Hokkaido University. This work was also supported by JST ERATO-FS Grant No. JP-MJER2105 and KAKENHI (Grants No. JP18J20727, No. JP18H01140, No. JP19K03646, No. 20H01828, No. 20H01828, No. JP20H01845, and No. JP21H01005).

Appendix A: Calculation of topological invariants

In this appendix, we derive the topological invariant in Eq. (29) by applying the method in Ref. [12]. At first, we construct the vectors $|\phi_n^\pm\rangle$ and $|\phi_n^\pm\rangle\rangle$ given in Eq.

(27). Let $|\psi_n\rangle$ and $|\psi_n\rangle\rangle$ be a right and left biorthonormal eigenvectors of $Z'(k)$,

$$Z'(k)|\psi_n\rangle = \lambda_n|\psi_n\rangle, \quad Z'^\dagger(k)|\psi_n\rangle\rangle = \lambda_n^*|\psi_n\rangle\rangle, \quad (\text{A1})$$

respectively. Suppose Z' has pseudo-Hermiticity $Z'(k) = \eta Z'^\dagger(k)\eta^{-1}$, then right and left eigenvectors are connected as

$$\eta|\psi_n\rangle\rangle = \sum_m A_{mn}|\psi_m\rangle \quad (\text{A2})$$

holds. Since $A = [A_{mn}]$ is Hermitian, A is diagonalized by a unitary matrix G

$$G^\dagger AG = \text{diag}\{\xi_1, \xi_2, \dots, \xi_N\}, \quad (\text{A3})$$

where $\xi_i \in \mathbb{R}$. By using the matrix G , biorthonormal vectors $|\phi_n^\pm\rangle$ and $|\phi_n^\pm\rangle\rangle$ are constructed as

$$|\phi_n\rangle := \sum_m \sqrt{|\xi_n|} G_{mn} |\psi_m\rangle, \quad (\text{A4})$$

$$|\phi_n\rangle\rangle := \sum_m \frac{G_{mn}}{\sqrt{|\xi_n|}} |\psi_m\rangle\rangle. \quad (\text{A5})$$

Then the state space is divided into two subsectors, one of which is spanned by states with

$$\eta|\phi_n\rangle = |\phi_n\rangle \quad (\text{A6})$$

and the other is spanned by states with

$$\eta|\phi_n\rangle = -|\phi_n\rangle\rangle. \quad (\text{A7})$$

We denote the former $|\phi_n^+\rangle$ ($|\phi_n^+\rangle\rangle$), and the latter $|\phi_n^-\rangle$ ($|\phi_n^-\rangle\rangle$).

The eigenvectors of $Z'(k)$ are given by

$$|\psi_{p,q}(k)\rangle = \frac{1}{2} \begin{pmatrix} \frac{(-1)^q}{\lambda_p'} [(-1)^{p+1}t_k^* + i\gamma^2] \\ (-1)^{p+1}i \\ \frac{(-1)^q}{\lambda_p'} [it_k^* + (-1)^p\gamma^2] \\ 1 \end{pmatrix}, \quad (\text{A8})$$

$$|\psi_{p,q}(k)\rangle\rangle = \frac{1}{2} \begin{pmatrix} \frac{(-1)^q}{\lambda_p'} [(-1)^{p+1}t_k^* - i\gamma^2] \\ (-1)^{p+1}i \\ \frac{(-1)^q}{\lambda_p'} [it_k^* + (-1)^{p+1}\gamma^2] \\ 1 \end{pmatrix}, \quad (\text{A9})$$

$$\lambda'_p := \sqrt{|t_k|^2 - \gamma^4 + (-1)^{p+1}2i\gamma^2\text{Ret}_k}. \quad (\text{A10})$$

Then the vectors $|\phi_n^\pm(k)\rangle$ and $|\phi_n^\pm(k)\rangle\rangle$ ($n \in \{0, 1\}$) are calculated as

$$|\phi_n^+(k)\rangle = \frac{1}{\sqrt{2}}(|\psi_{0,n}(k)\rangle + i|\psi_{1,n}(k)\rangle), \quad (\text{A11})$$

$$|\phi_n^+(k)\rangle\rangle = \frac{1}{\sqrt{2}}(|\psi_{0,n}(k)\rangle\rangle + i|\psi_{1,n}(k)\rangle\rangle), \quad (\text{A12})$$

$$|\phi_n^-(k)\rangle = \frac{1}{\sqrt{2}}(-|\psi_{0,n}(k)\rangle + i|\psi_{1,n}(k)\rangle), \quad (\text{A13})$$

$$|\phi_n^-(k)\rangle\rangle = \frac{1}{\sqrt{2}}(-|\psi_{0,n}(k)\rangle\rangle + i|\psi_{1,n}(k)\rangle\rangle). \quad (\text{A14})$$

By using the projection operators onto plus and minus subsectors,

$$P^\pm(k) := \sum_n |\phi_n^\pm(k)\rangle \langle\langle \phi_n^\pm(k)|. \quad (\text{A15})$$

Each subsection of the matrix Z' is provided as

$$Z'_\pm(k) := P^\pm(k)Z'(k)P^\pm(k), \quad (\text{A16})$$

and their explicit expressions are given as

$$Z'_\pm(k) = \pm \frac{\lambda_{0,0}(k) + \lambda_{1,0}(k)}{2} (|\phi_0^\pm(k)\rangle \langle\langle \phi_0^\pm(k)| - |\phi_1^\pm(k)\rangle \langle\langle \phi_1^\pm(k)|) \quad (\text{A17})$$

where $\lambda_{p,q}(k)$ is the eigenvalue of Z given in Eq. (20). Z'_\pm has SLS $Z'_\pm(k) = -\mathcal{S}_\pm Z'_\pm(k)\mathcal{S}_\pm^{-1}$, $\mathcal{S}_\pm = I_2 \otimes \sigma_z$, thus we can define the winding numbers in Eq. (28) for each

subsector. We have

$$\begin{aligned} & \text{tr} \left[\mathcal{S}_\pm Z'_\pm(k) \frac{dZ'_\pm(k)}{dk} \right] \\ &= -2 \left(\langle\langle \phi_1^\pm(k) | \frac{d\phi_0^\pm(k)}{dk} \rangle\rangle - \langle\langle \phi_0^\pm(k) | \frac{d\phi_1^\pm(k)}{dk} \rangle\rangle \right) \quad (\text{A18}) \end{aligned}$$

After some algebra using Eqs. (A8)~(A14), we get

$$\begin{aligned} & \text{tr} \left[\mathcal{S}_+ Z'_+(k) \frac{dZ'_+(k)}{dk} \right] = \text{tr} \left[\mathcal{S}_- Z'_-(k) \frac{dZ'_-(k)}{dk} \right] \\ &= \frac{d}{dk} [\log(t_k^* - i\gamma^2) + \log(t_k^* - i\gamma^2) - \log \lambda_0' - \log \lambda_0'^*]. \quad (\text{A19}) \end{aligned}$$

In our model λ_0' does not have winding number, thus $\frac{1}{2\pi i} \int_{\text{BZ}} dk \frac{d}{dk} \log \lambda_0' = \frac{1}{2\pi i} \int_{\text{BZ}} dk \frac{d}{dk} \log \lambda_0'^* = 0$ holds. Then we have $w_+ = w_-$ and they are given as

$$w_\pm = \frac{1}{4\pi i} \int_{\text{BZ}} dk \left[\frac{d}{dk} \log(t_k^* - i\gamma^2) + \frac{d}{dk} \log(t_k^* + i\gamma^2) \right]. \quad (\text{A20})$$

As a result, the topological invariant for Z is given as $w = w_+ + w_-$ and is provided as Eq. (29).

[1] K. Esaki, M. Sato, K. Hasebe, and M. Kohmoto, Phys. Rev. B **84**, 205128 (2011).
[2] T. E. Lee, Phys. Rev. Lett. **116**, 133903 (2016).
[3] S. Lieu, Phys. Rev. B **97**, 045106 (2018).
[4] K. Kawabata, Y. Ashida, H. Katsura, and M. Ueda, Phys. Rev. B **98**, 085116 (2018).
[5] K. Yokomizo and S. Murakami, Phys. Rev. Lett. **123**, 066404 (2019).
[6] T. Liu, Y.-R. Zhang, Q. Ai, Z. Gong, K. Kawabata, M. Ueda, and F. Nori, Phys. Rev. Lett. **122**, 076801 (2019).
[7] Q.-B. Zeng, Y.-B. Yang, and Y. Xu, Phys. Rev. B **101**, 020201 (2020).
[8] Y. Ashida, Z. Gong, and M. Ueda, Adv. Phys. **69**, 249 (2020).
[9] E. J. Bergholtz, J. C. Budich, and F. K. Kunst, Rev. Mod. Phys. **93**, 015005 (2021).
[10] Z. Gong, Y. Ashida, K. Kawabata, K. Takasan, S. Higashikawa, and M. Ueda, Phys. Rev. X **8**, 031079 (2018).
[11] K. Kawabata, S. Higashikawa, Z. Gong, Y. Ashida, and M. Ueda, Nat. Commun. **10**, 1 (2019).
[12] K. Kawabata, K. Shiozaki, M. Ueda, and M. Sato, Phys. Rev. X **9**, 041015 (2019).
[13] S. Yao and Z. Wang, Phys. Rev. Lett. **121**, 086803 (2018).
[14] N. Okuma, K. Kawabata, K. Shiozaki, and M. Sato, Phys. Rev. Lett. **124**, 086801 (2020).
[15] M. Kawasaki, K. Mochizuki, N. Kawakami, and H. Obuse, Prog. Theor. Exp. Phys. **2020**, 12A105 (2020).
[16] K. Zhang, Z. Yang, and C. Fang, Phys. Rev. Lett. **125**, 126402 (2020).
[17] K. Sone, Y. Ashida, and T. Sagawa, Nat. Commun. **11**, 1 (2020).
[18] S. Weimann, M. Kremer, Y. Plotnik, Y. Lumer, S. Nolte, K. G. Makris, M. Segev, M. C. Rechtsman, and A. Szameit, Nat. Mater. **16**, 433 (2017).
[19] M. A. Bandres, S. Wittek, G. Harari, M. Parto, J. Ren, M. Segev, D. N. Christodoulides, and M. Khajavikhan, Science **359** (2018).
[20] K. Mochizuki, D. Kim, and H. Obuse, Phys. Rev. A **93**, 062116 (2016).
[21] L. Xiao, X. Zhan, Z. H. Bian, K. K. Wang, X. Zhang, X. P. Wang, J. Li, K. Mochizuki, D. Kim, N. Kawakami, W. Yi, H. Obuse, B. C. Sanders, and P. Xue, Nat. Phys. **13**, 1117 (2017).
[22] L. Xiao, T. Deng, K. Wang, G. Zhu, Z. Wang, W. Yi, and P. Xue, Nature Physics **16**, 761 (2020).
[23] H.-P. Breuer and F. Petruccione, *The theory of open quantum systems* (Oxford University Press on Demand, 2002).
[24] G. T. Landi, D. Poletti, and G. Schaller, arXiv preprint arXiv:2104.14350 (2021).
[25] T. Prosen, Phys. Rev. Lett. **106**, 217206 (2011).
[26] F. Minganti, A. Biella, N. Bartolo, and C. Ciuti, Phys. Rev. A **98**, 042118 (2018).
[27] T. Mori and T. Shirai, Phys. Rev. Lett. **125**, 230604 (2020).
[28] L. Sá, P. Ribeiro, and T. Prosen, Phys. Rev. X **10**, 021019 (2020).
[29] T. Haga, M. Nakagawa, R. Hamazaki, and M. Ueda, Phys. Rev. Lett. **127**, 070402 (2021).
[30] M. Nakagawa, N. Kawakami, and M. Ueda, Phys. Rev. Lett. **126**, 110404 (2021).
[31] S. Diehl, E. Rico, M. A. Baranov, and P. Zoller, Nat. Phys. **7**, 971 (2011).

- [32] C.-E. Bardyn, M. A. Baranov, C. V. Kraus, E. Rico, A. İmamoğlu, P. Zoller, and S. Diehl, *New J. Phys.* **15**, 085001 (2013).
- [33] J. C. Budich, P. Zoller, and S. Diehl, *Phys. Rev. A* **91**, 042117 (2015).
- [34] D.-J. Zhang and J. Gong, *Phys. Rev. A* **98**, 052101 (2018).
- [35] A. Altland, M. Fleischhauer, and S. Diehl, *Phys. Rev. X* **11**, 021037 (2021).
- [36] V. P. Flynn, E. Cobanera, and L. Viola, *Phys. Rev. Lett.* **127**, 245701 (2021).
- [37] F. Dangel, M. Wagner, H. Cartarius, J. Main, and G. Wunner, *Phys. Rev. A* **98**, 013628 (2018).
- [38] M. van Caspel, S. E. T. Arze, and I. P. Castillo, *SciPost Phys.* **6**, 26 (2019).
- [39] F. Song, S. Yao, and Z. Wang, *Phys. Rev. Lett.* **123**, 170401 (2019).
- [40] M. Goldstein, *SciPost Phys.* **7**, 067 (2019).
- [41] S. Lieu, M. McGinley, and N. R. Cooper, *Phys. Rev. Lett.* **124**, 040401 (2020).
- [42] T. Yoshida, K. Kudo, H. Katsura, and Y. Hatsugai, *Phys. Rev. Research* **2**, 033428 (2020).
- [43] Y.-W. Huang, P.-Y. Yang, and W.-M. Zhang, *Phys. Rev. B* **102**, 165116 (2020).
- [44] S. Longhi, *Phys. Rev. B* **102**, 201103 (2020).
- [45] J.-S. Pan, L. Li, and J. Gong, *Phys. Rev. B* **103**, 205425 (2021).
- [46] T. Prosen, *Phys. Rev. Lett.* **109**, 090404 (2012).
- [47] B. Buća and T. Prosen, *New J. Phys.* **14**, 073007 (2012).
- [48] V. V. Albert and L. Jiang, *Phys. Rev. A* **89**, 022118 (2014).
- [49] M. van Caspel and V. Gritsev, *Phys. Rev. A* **97**, 052106 (2018).
- [50] J. Huber, P. Kirton, S. Rotter, and P. Rabl, *SciPost Phys.* **9**, 52 (2020).
- [51] S. Lieu, R. Belyansky, J. T. Young, R. Lundgren, V. V. Albert, and A. V. Gorshkov, *Phys. Rev. Lett.* **125**, 240405 (2020).
- [52] T. Prosen, *New J. Phys.* **10**, 043026 (2008).
- [53] T. Prosen, *J. Stat. Mech.* **2010**, P07020 (2010).
- [54] W.-P. Su, J. Schrieffer, and A. Heeger, *Phys. Rev. B* **22**, 2099 (1980).
- [55] A. Y. Kitaev, *Phys. Usp.* **44**, 131 (2001).
- [56] We note that the eigenvectors of Z are not proper quantum states in general because ρ_j in Eq. (3) are not Hermitian when $\text{Re } \nu_j \neq 0$. However, we call the eigenvectors as "states" to adapt to the convention of topological matters.